SOLID SOLUBILITY OF MAGNESIUM IN THE CLOSE-PACKED MODIFICATIONS OF SOME RARE EARTH METALS

by

Robert Roderick Joseph

A Thesis Submitted to the
Graduate Faculty in Partial Fulfillment of
The Requirements for the Degree of
MASTER OF SCIENCE

Major Subject: Metallurgy

Iowa State University
Of Science and Technology
Ames, Iowa

1965

TABLE OF CONTENTS

I. INTRODUCTION

A. General

The existence of solid solutions has been known since the studies of Matthiessen in 1860. In 1900 Gibbs and his phase rule firmly established solid solutions as an important concept in chemistry and metallurgy. Much of the early theory of solid solutions was worked out in the 1930's by Jones, Hume-Rothery, Rushbrook, Guggenhiem and others. Since the 1930's large numbers of systems have been found in which the components have some solubility in each other. During the last fifteen years more powerful experimental tools have been used to probe at the electronic and spatial structure of solid solutions.

This introduction will serve to explain the nature of solid solutions and briefly summarize some of the theories which attempt to explain the structure and properties of solid solutions. There are two types of solid solutions which occur, interstitial and substitutional. The interstitial is characterized by the solute atom existing in the interstices between atoms while in the substitutional case the solute atoms replace solvent atoms on their lattice sites. This work is concerned only with substitutional solid solutions since

interstitial solutions occur only with solutes of very small atomic diameter.

The early workers believed that for the most part solid solutions consisted of a random distribution of solute atoms on the solvents lattice sites. More recent work has shown that a random distribution of solute atoms is the exception and that clustering or ordering is usually the rule (1, p. 201). Clustering is defined as an atom having more like atoms as nearest neighbors than in the random case and ordering as the case where there are fewer like atoms as nearest neighbors.

One effect of forming a solid solution is the change in lattice dimensions which usually occurs because the size of the solute is significantly different from that of the solvent. In the following discussion the atom size referred to will be that calculated from lattice parameter measurements using a hard sphere model and correcting for coordination. Vegard (2) in his work on ionic salts observed a relation which he thought applied to all solid solutions. Vegard's "law" states that if atoms of different sizes are mixed the resulting lattice parameter of the alloy would be a weighted average of the two sizes. Experimentally Vegard's "law" has been shown to hold true in only a very few cases. In other

words experiments have shown that when atoms of different sizes are alloyed the atoms change size. The apparent size of the solute atom may be determined by an extrapolation of the lattice parameter versus composition curve to 100% solute. The resulting atom size, called the apparent atomic radius, will be the pure metal radius of the solute if Vegard's "law" holds, or as usually is the case the radius will be larger or smaller than the pure metal radius.

B. Elasticity Theories

The elastic model of a solid solution as proposed by Friedel (3) permits one to predict the magnitude and sign of the deviation from Vegard's "law". This model considers the solid as an elastic continuum in which a spherical hole of radius r_1 is made (r_1 = radius of solvent, r_2 = radius of solute). The sphere of radius r_2 with the elastic properties of the solute is placed in the void and joined to the matrix so that it either expands or contracts depending on the sign of $r_2 - r_1$ and the compressibilities of the solute and solvent. Friedel's equation for deviations from Vegard's "law" is

$$r - r_v = c_2 \frac{(\varkappa_1/\varkappa_2 - 1)(r_2 - r_1)}{(\alpha + 1)}$$

where $\alpha = \frac{(1+\nu)\chi_1}{2(1-2\nu)\chi_2}$

r = radius of alloy

r_v = radius of alloy from Vegard's "law"

χ_1 = compressibility of solvent atom

χ_2 = compressibility of solute atom

ν = Poisson's ratios for solvent

c_2 = concentration of component 2.

By using Friedel's equation it is possible to make an extrapolation to 100% solute to obtain an apparent atomic diameter due to first order elasticity theory (4).

The second order elasticity theory effect assumes that the volume change in the model is not zero as predicted by first order elasticity (5). Therefore a further deviation from Vegard's "law" can be calculated $r - r_v = 2\left(\frac{d\mu_1}{dp} - \frac{\mu_1}{B_1}\right)\frac{(r_1 - r_2)^2}{r_1} c_2$

where μ_1 = shear modulus

p = pressure

B_1 = bulk modulus

and $\left(\frac{d\mu_1}{dp} - \frac{\mu_1}{B_1}\right) = 2\frac{\mu_1}{B_1}\gamma_1$

where γ_1 = Grüneisen constant.

From the above mentioned theories one would expect the size of the atoms to be important in the formation of solid solutions. If the difference in atom size is large the strain energy of the lattice will be high and solid solution may dissociate into a lower energy configuration (2 phase alloy). That this will occur was postulated empirically by Hume-Rothery (6, p. 100). The first of Hume-Rothery rules, the size factor, states that if the atoms differed in size by more than 15% extensive solid solutions would not form. Rider (4) has shown for gold-rare earth solid solutions that the solubility of the rare earth metals increases as the size factor becomes less than 15%. A theoretical basis for this 15% value was derived independently by Eshelby (7) and Friedel (8) by using a combination of first order elasticity and quasi-chemical approaches.

C. Electronic Theories

An important effect in the formation of solid solutions is the interaction of the electrons of the solute and solvent atoms. The remaining Hume-Rothery rules (6, p. 104) are related to electronic effects and are stated as follows: the greater the difference in the electrochemical properties

between solvent and solute and more restricted the solid solubility will be; and a metal of lower valence will dissolve more readily a metal of higher valency than vice-versa. If atoms have widely different electrochemical properties there will be a strong tendency to form compounds and from free energy diagrams it can be seen that this will restrict solubility. Other theories on electrical effects due to Friedel (8) and Jones (9) deal with the effect of solute atoms in perturbing the electric field of the lattice. These theories attempt to picture what happens to the band structure of a metal when an excess or deficiency of electrons is added by a solute of different valency than the solvent.

It was mentioned above that the Hume-Rothery rule predicted no solubility if the size factor was greater than 15%, but the rule does not guarantee that there will be significant solubility if the size factor is less than 15%. Because of other conditions like the difference in electronegativities solid solubility may be severely restricted. Darken and Gurry (10, p. 86) have attempted to combine these two effects by plotting size of an atom versus its electronegativity. They obtain a plot with a series of points on it each representing an element. An ellipse with a minor axis of $\pm$ 15% of the

radius of the solvent and a major radius of ± .4 units in electronegativity is then drawn around the solvent. The elements that are expected to be more than 5% soluble in the chosen solvent lie within the ellipse. For those elements which lie outside the ellipse the solubility is expected to be less than 5 atomic percent. Waber et al. (11) have shown that for 62 elements this method is 76.6% correct in its predictions of whether or not extensive solubility occurs.

Hume-Rothery et al. (12) observed that most copper, silver, and gold solid solutions appeared to have phase boundaries at constant electron to atom ratios. According to Jones (9) the stable phase of an alloy will be determined by the crystal structure which will accomodate additional electrons with the smallest increase in energy (i.e. the highest density of states curve). Jones showed that if a spherical Fermi surface was assumed the face centered cubic lattice became unstable with respect to the body centered cubic lattice at values of the electron to atom ratio which agreed with those determined experimentally. More recent experimental work by Pippard (13) and other experimental work reviewed by Massalski and King (14) show that in pure copper the Fermi surface is not spherical and in fact it is already

in contact with the first Brillouin zone. Therefore Jones' theory is probably incorrect as originally stated but the experimental fact that the phase boundaries occur at a constant electron to atom ratio is too conclusive to be considered coincidental.

D. Statistical Theories

The quasi-chemical theories attempt to explain heats of formation and entropies of formation based on a consideration of nearest neighbor atoms. The theory assumes that the energy of the AA, BB, and AB bonds remains constant on alloying and that the distribution of B atoms on lattice sites is independent of its neighbors. The theory enables one to determine the sign and magnitude of the excess entropy and the enthalpy if the sign and magnitude of the short range order parameters are known (15).

Since no diffuse x-ray scattering data or enthalpy data are available for the systems of interest in this paper these theories will not be considered further.

E. Present Study

This study of the solubility of magnesium in the trivalent rare earth metals was initiated because the valency

contribution is held constant and the electrochemical contribution (as given by the electronegativity) is essentially constant and it is possible to examine the effect of the size factor on the solubility. The size factors based on pure metal radii range from 14.6% for lanthanum to 7.5% for lutetium. The electronegativity difference is small, 0.06 units or less, so that on a Darken and Gurry plot for solvent lanthanum the magnesium point falls just inside the ellipse.

For the rest of the rare earth solvents, the magnesium point moves closer to the solvent point (center of ellipse) as the atomic number increases, indicating that the solubility of magnesium would be expected to increase as we proceed along the rare earth series. In contrast application of the Jones theory (i.e. maximum solubility occurs at constant electron concentration) to these polyvalent solvents and solute indicate that the solubility would be expected to be constant across the series. A search of the literature revealed no data on the solubility of magnesium in the rare earths with the exception of one point for the Ce-Mg system by Gschneidner (16). The value of the eutectoid and peritectic temperatures of the heavy rare earths (17), lanthanum (18), cerium (19), and praseodymium (20) were obtained from

the literature. The phase diagrams for the rare earth rich end of the RE-Mg systems appear to be similar and a representative diagram is shown in Figure 1. (RE = rare earth)

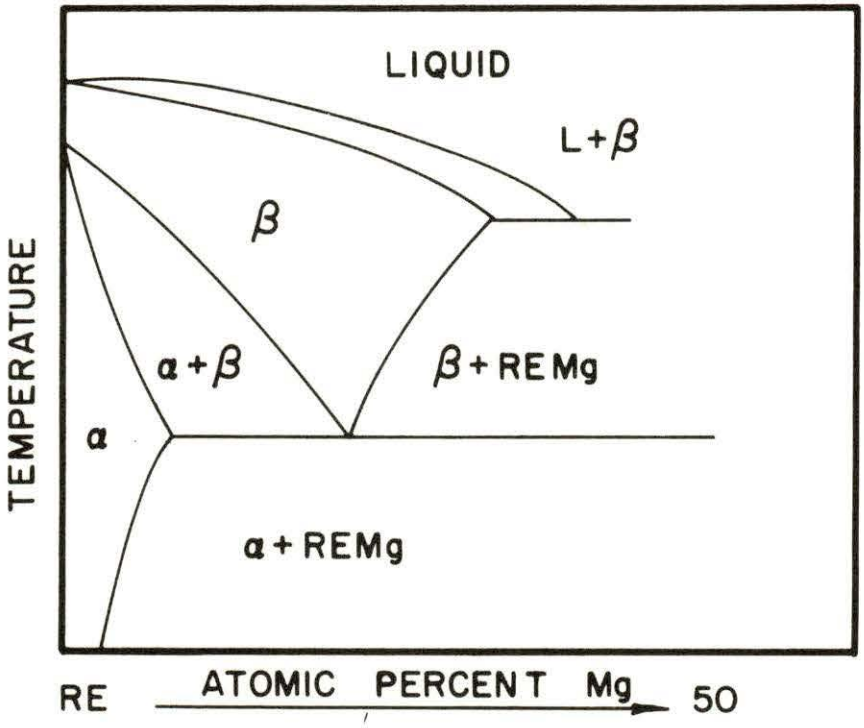

Figure 1. Approximate phase diagram for rare earth rich end of rare earth-magnesium phase diagram

II. PROCEDURES

A. Materials

The rare earth metals used in the preparation of alloys for this investigation were prepared from rare earth oxides by metallothermic reduction techniques previously described by Daane (21, p. 102). The techniques used in the reduction of the oxides and in the preparation of the metal are considered to be the best available at the present time. The chemical analyses of the metals used are listed in Table 1. The magnesium used in this investigation had been double distilled and it contained the impurities listed in Table 1.

B. Preparation of Alloys

The rare earth-magnesium alloys were prepared by placing the weighed components in outgassed tantalum crucibles. The rare earth metals were buffed on a wire wheel just prior to weighing to remove any oxide coating. The crucibles were sealed under an atmosphere of helium by welding on a tantalum lid. The total weight of the alloys was 5 to 7 grams.

For the alloys prepared from the rare earth metals which melted below 1000°C (La, Ce, Pr, Nd) the crucibles were sealed in evacuated quartz tubing and held for 24 hrs in

Table 1. Analysis of rare earth metals and magnesium (ppm)

	La	Ce	Pr	Nd	Gd	Dy	Lu	Mg
H_2	20	<5	<5	4	<5	32	65	
C								70
N_2	100	11	61	44	21	3	282	
O_2	350	183	508	287	613	158	937	
Si	<50	15	<500	50	10	20	<15	FT
Ca	10	<50	<200	100	5	<300	16	T
Fe	<5	<50	30	100	75	100	<25	<10
Ni								FT
Cu								FT
Y					$\bar{<}$20	<10	<100	
La		$\bar{<}$200	$\bar{<}$50					
Ce	$\bar{<}$300		<<1000					
Pr	$\bar{<}$300	$\bar{<}$200		<1000				
Nd	$\bar{<}$200	$\bar{<}$200	<600					
Sm				<100	$\bar{<}$200			
Eu					$\bar{<}$10			
Gd						<200		
Tb					$\bar{<}$100	<1000		
Dy								
Ho						<100		
Er						<450	<10	
Tm							<10	
Yb							50	
Ta	$\bar{<}$200	<1000	500	<500	500	400	500	

resistance furnaces at 50 to 100°C above the melting point of the rare earth metals. For the higher melting rare earth metals the sealed crucibles were heated in vacuum induction furnaces at temperatures of 50 to 100°C above the melting point of the pure rare earth metals for 15 to 30 minutes. All specimens except lutetium-magnesium were homogenized for 200 hours or more at a temperature a few degrees below the eutectoid transformation temperature. Because of the low eutectoid temperature of lutetium in comparison to its melting point the lutetium alloys were first held at 1000°C for 48 hours then held at the eutectoid temperature for 200 hours. After the samples were heat treated for the appropriate length of time they were water quenched. After quenching the tantalum was removed from the specimens by mechanical stripping or machining. Several alloys were examined metallographically for evidence of macrosegregation but none was observed.

C. Preparation of X-ray Sample

Filings were taken from the entire cross section of the specimens by use of a six inch file. A new file surface was used for each alloy to prevent contamination. The particle size of the filings was found to be small enough to give

smooth diffraction lines without using screens. The filings were placed in small tantalum capsules (made from 1/8" tubing) and the ends of the capsules were welded shut. The filing of the alloys was done in air for lutetium, dysprosium, gadolinium, neodymium and praseodymium but the cerium and lanthanum alloys were filed in a dry box under an argon atmosphere to prevent contamination. Some of the neodymium and praseodymium alloys were filed in the dry box but no difference in the x-ray patterns as compared with those alloys filed in air could be detected. Therefore, it was concluded that none of the alloys filed in air were oxidized or otherwise contaminated. The filings of the rare earth alloys were annealed for convenient lengths of time to establish equilibrium. In the range 200-400°C the filings were annealed 48 hours, in the range 400-500°C, 24 hours. These times represent minimums.

Because of the high vapor pressure of magnesium above 550°C, alloys of gadolinium and dysprosium were annealed as ingots and then the filings were given a stress relief anneal for 5 minutes at the same temperature that the ingot was annealed. This was done only for temperatures above 550°C because preliminary experiment showed that a change of

lattice parameter with increasing annealing time occurred above 550°C indicating a loss of magnesium from the filings. Attempts to calculate the composition change expected from known vapor pressure data of Ogren (22) indicated that no significant weight loss would be expected unless the magnesium vapor combined with the tantalum, either by chemical reaction (very unlikely) or by absorption on the tantalum surface.

The filings were placed in 0.3 mm wall commercial x-ray capillaries. The capillaries containing heavy rare earth alloys were sealed in air and those containing light rare earth alloys were sealed under a 10 micron vacuum.

D. Determination of Solubility

The solubility of magnesium in the rare earth metals was determined from the lattice parameters of the alloys in the following manner. It is found that the lattice parameter of most binary alloys is a function of composition in the one phase region but in the two phase region the lattice parameter is constant because of the constant composition of the phases at any given temperature. It is, therefore, possible to establish a lattice parameter versus composition curve at

room temperature by quenching alloys from the single phase region and measuring their lattice parameter at room temperature. Alloys of constant composition when quenched from any temperature within the one phase region will have the same lattice parameter. Conversely alloys of any composition in the two phase region quenched from a given temperature have the same lattice parameter. The lattice parameter then may be used to determine the maximum solubility at the given temperature from the lattice parameter versus composition curve.

The alloys of lanthanum, cerium and lutetium were examined using copper K_α radiation (K_{α_1} = 1.54050 Å) and the praseodymium, neodymium, gadolinium and dysprosium alloys were examined using chromium K_α radiation (K_{α_1} = 2.28962 Å). By using either radiation it was possible to obtain 4 to 8 lines (usually as K_{α_1}, K_{α_2}, doublets) in the back reflection region ($\theta > 60^\circ$). The lattice parameters were determined by measuring the diffraction line spacing from a 114.59 mm Debye-Scherrer camera. The line spacings from the film were extrapolated by using a Nelson-Riley or a $\phi\tan\phi$ extrapolation function with the aid of 7074 computer program.

E. Determination of Eutectoid Temperature

The eutectoid temperatures of several of the systems was measured using a differential thermal analysis (DTA) unit. The DTA apparatus consisted of a tantalum resistance heater containing a molybdenum block into which the sample in its tantalum crucible is placed. The heating and cooling rates used were 1°C/min., 2½°C/min. and 5°C/min. The thermocouple and differential thermocouple outputs were recorded on strip charts and the temperature of the thermal arrests were recorded on a potentiometer. The temperature of the thermal arrests is thought to be known to better than $\pm$ 2°C.

The eutectoid temperature for Nd-Mg alloys had not been previously determined and the solubility data on lanthanum and cerium indicated that the eutectoid temperature for these systems was probably in error. Therefore, the eutectoid temperature for these three systems was determined.

III. RESULTS

A. Eutectoid Temperature

The results of the determination of the eutectoid temperatures of lanthanum, cerium, and neodymium are given below.

	This work	Literature
Lanthanum-Magnesium	544 ± 2°C	530°C (18)
Cerium-Magnesium	505 ± 2°C	490°C (19)
Neodymium-Magnesium	551 ± 2°C	

In all cases the transformation temperature on heating was higher than that on cooling. As slower heating and cooling rates were used the transformation temperature on cooling began to rise but the temperature on heating remained constant. The values for the transformation temperature were taken to be those on heating since it appeared that the transformation temperature on cooling was being affected by supercooling. The difference between the present values and the literature is presumably due to difference in purity of the rare earth metals.

B. Lattice Parameter Versus Composition

Curves of lattice parameter versus composition were determined and are given in Figures 2 and 3. It was found

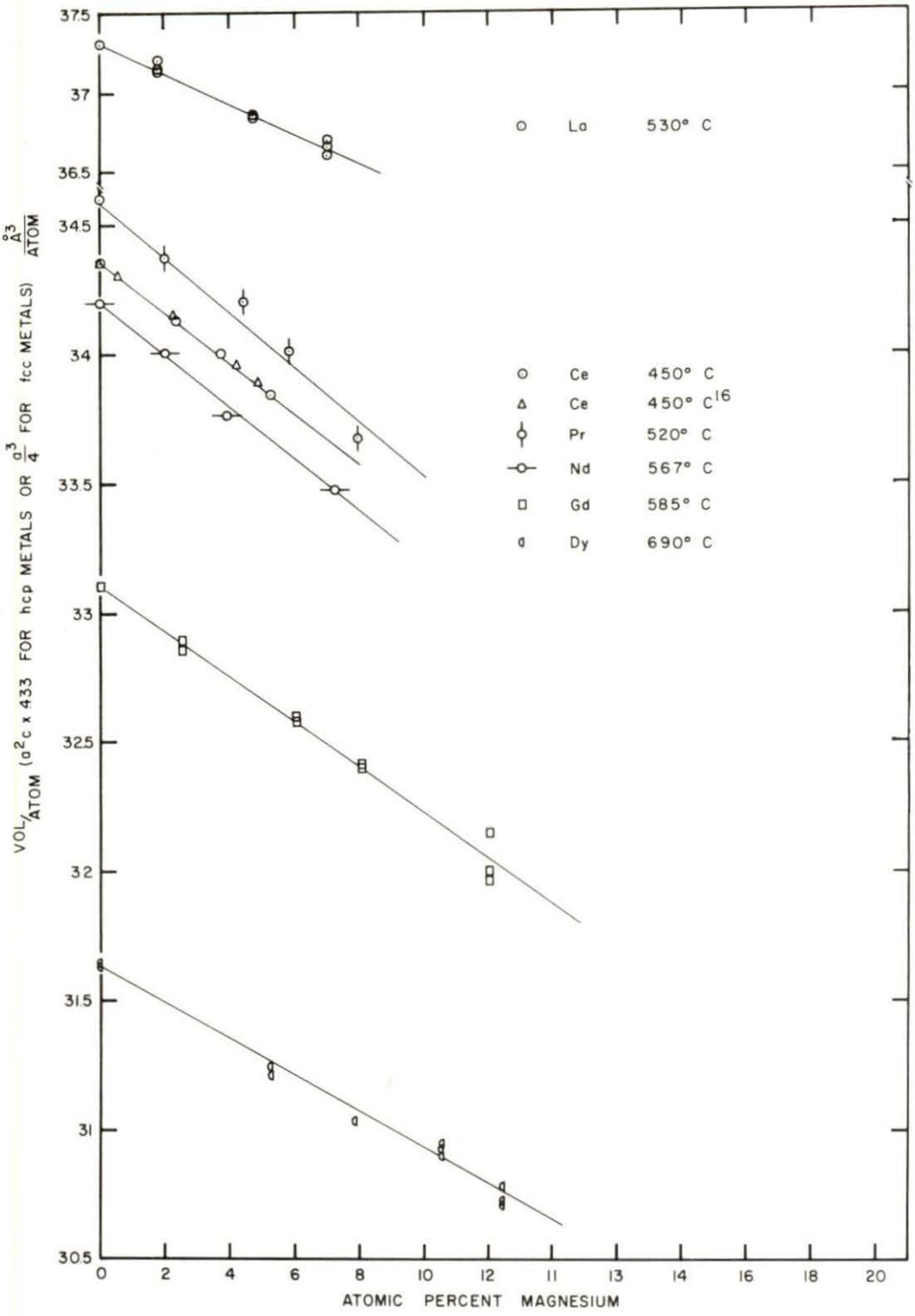

Figure 2. Volume per atom versus atomic percent magnesium for some of the rare earth metal

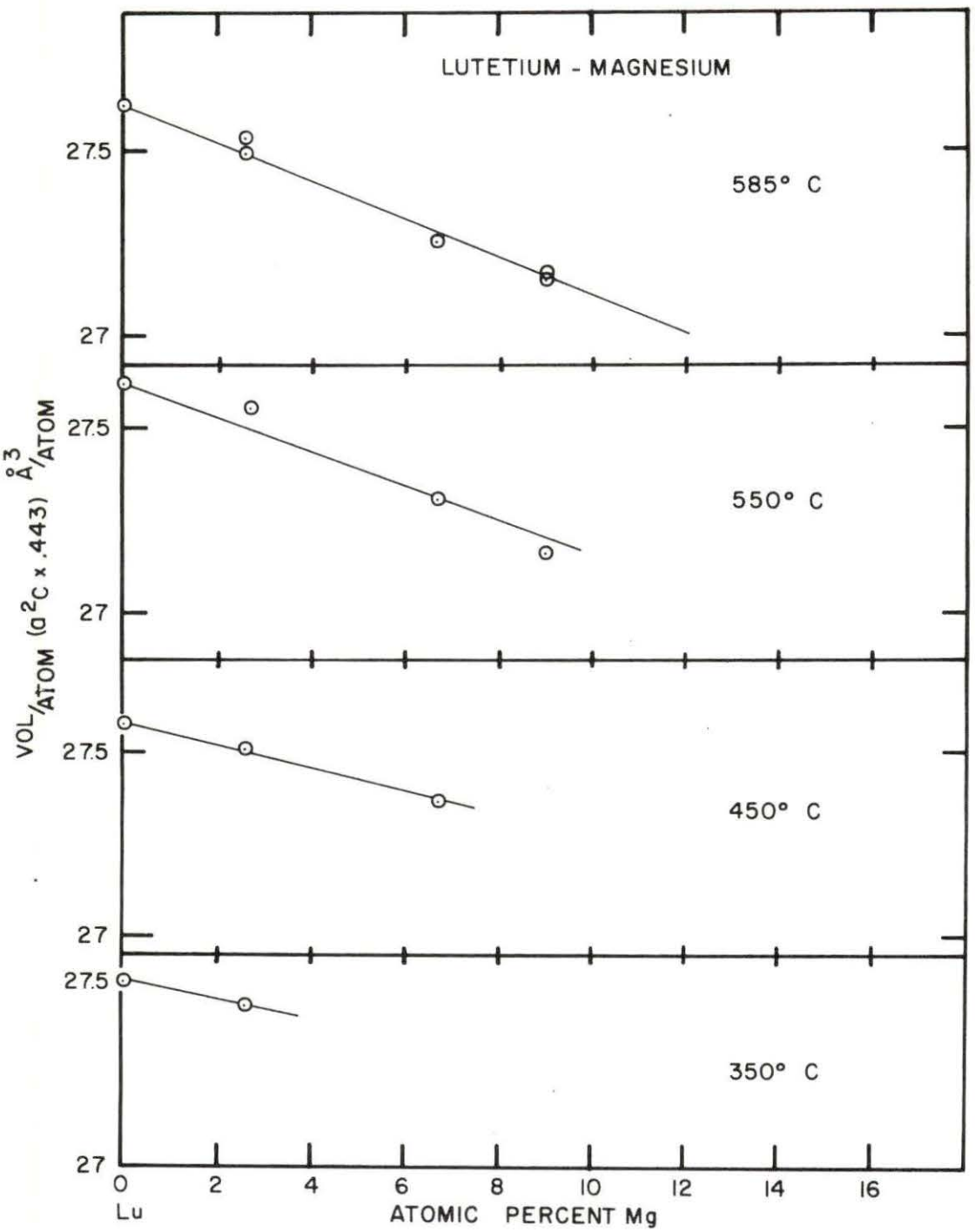

Figure 3. Volume per atom versus atomic percent magnesium in lutetium

that the variation of volume per atom ($\underline{a}^2\underline{c}$ x .433 for hcp) with composition was sensitive enough to determine values for the solubility. Plots of $\underline{a}_o$ versus composition and $\underline{c}_o$ versus composition were also made but they were not significantly different from the volume plots with the exception that the $\underline{c}_o$ plots had an increased amount of scatter. The plots of volume versus composition were independent of temperature with the exception of lutetium Figure 3. In lutetium a variation of lattice parameter with annealing temperature for the pure metal was observed (see section on errors). Therefore, the volume versus composition curve was determined at each temperature that the solubility was determined.

C. Solubility Data

The curves of solubility versus temperature are shown in Figures 4 to 8. They were determined from volume versus composition curves of alloys quenched from the temperatures of interest (Appendix).

The results of the solubility data may be summarized by a log solubility versus 1/T plot. Previous work has shown that when solubility data is plotted in this manner the resulting curve usually is linear. According to the Gibbs-

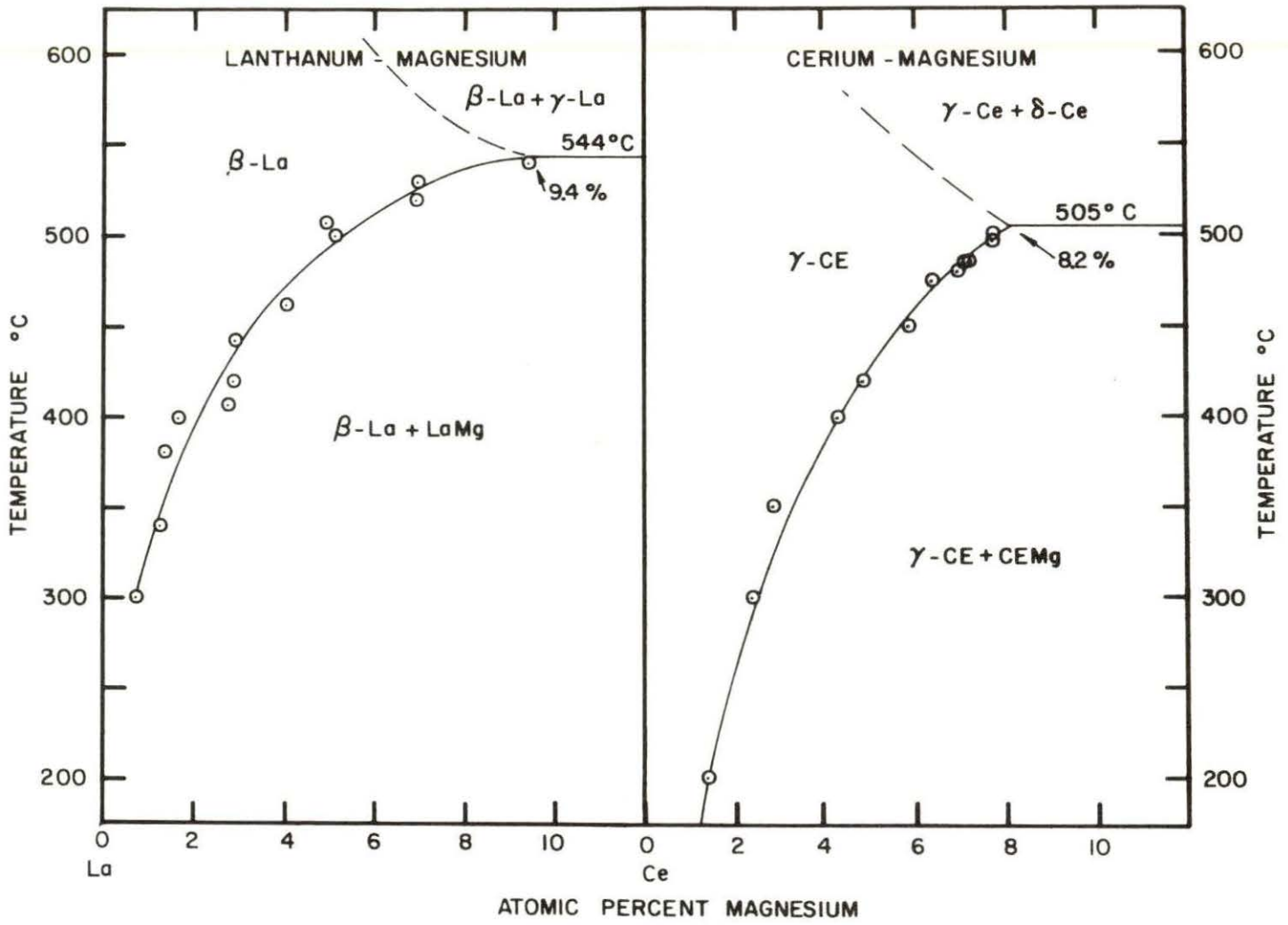

Figure 4. Phase diagrams for La-Mg, Ce-Mg systems showing solid solubility as a function of temperature

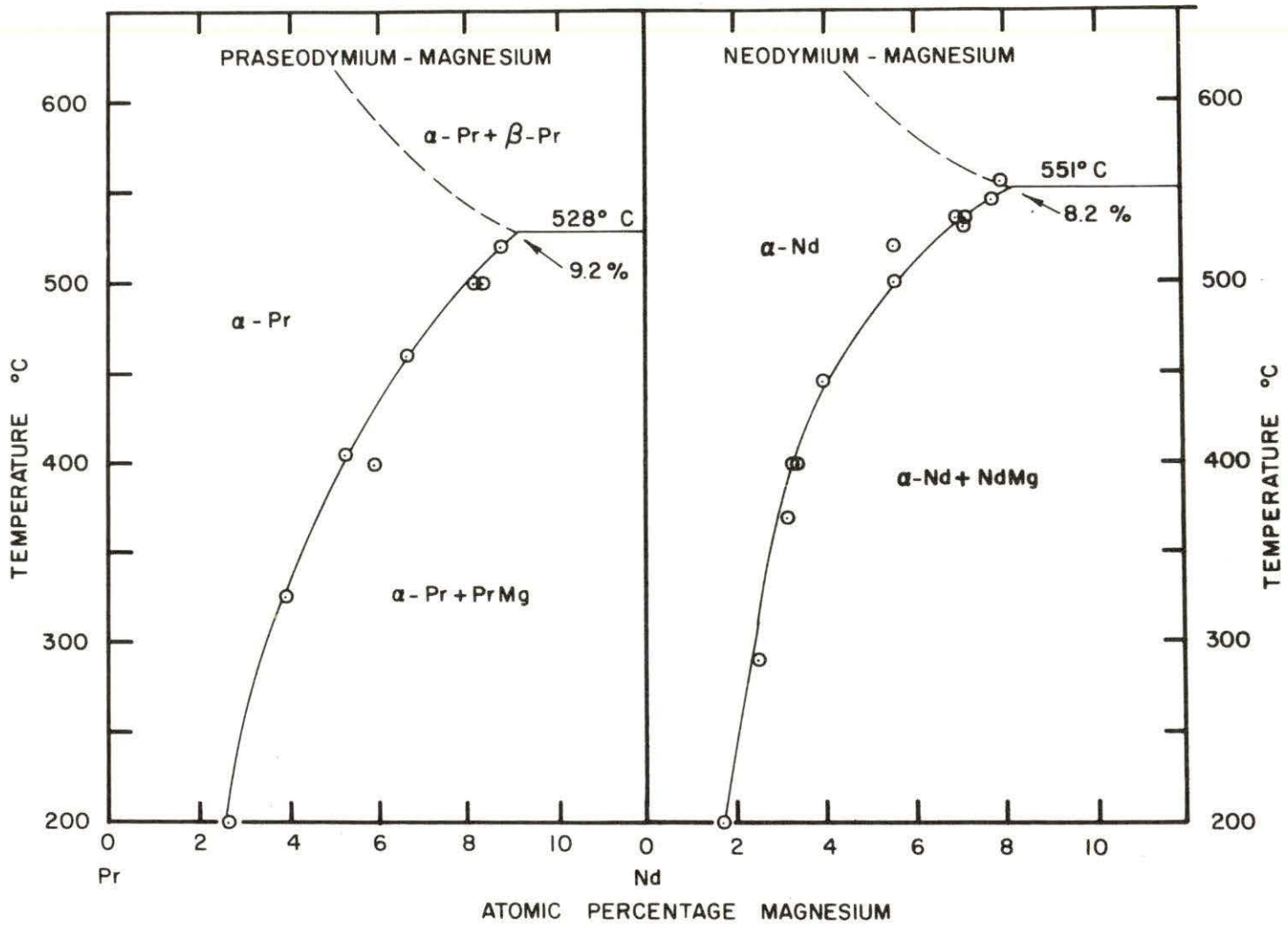

Figure 5. Phase diagrams for Pr-Mg, Nd-Mg systems showing solid solubility as a function of temperature

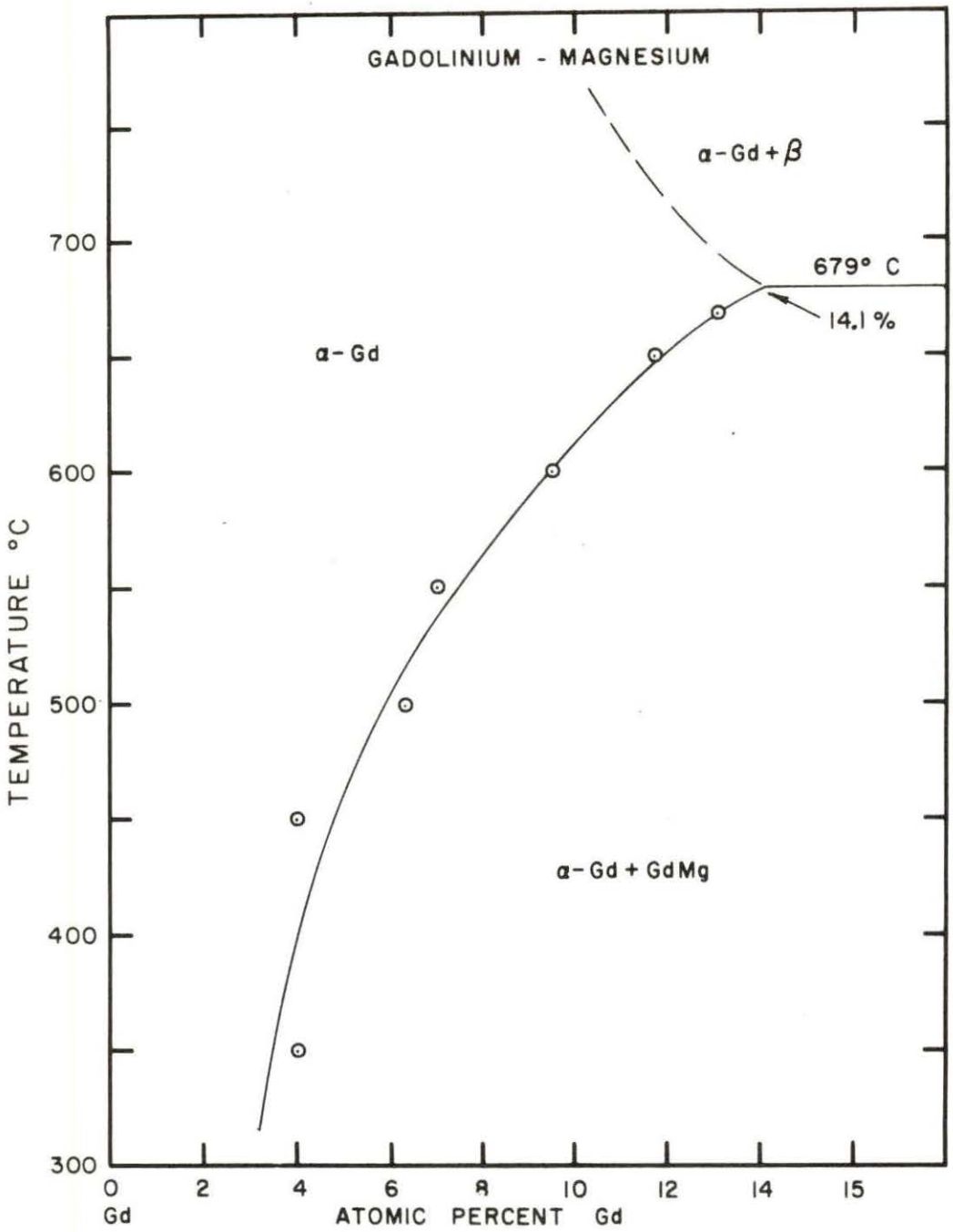

Figure 6. Phase diagram for Gd-Mg systems showing solid solubility as a function of temperature

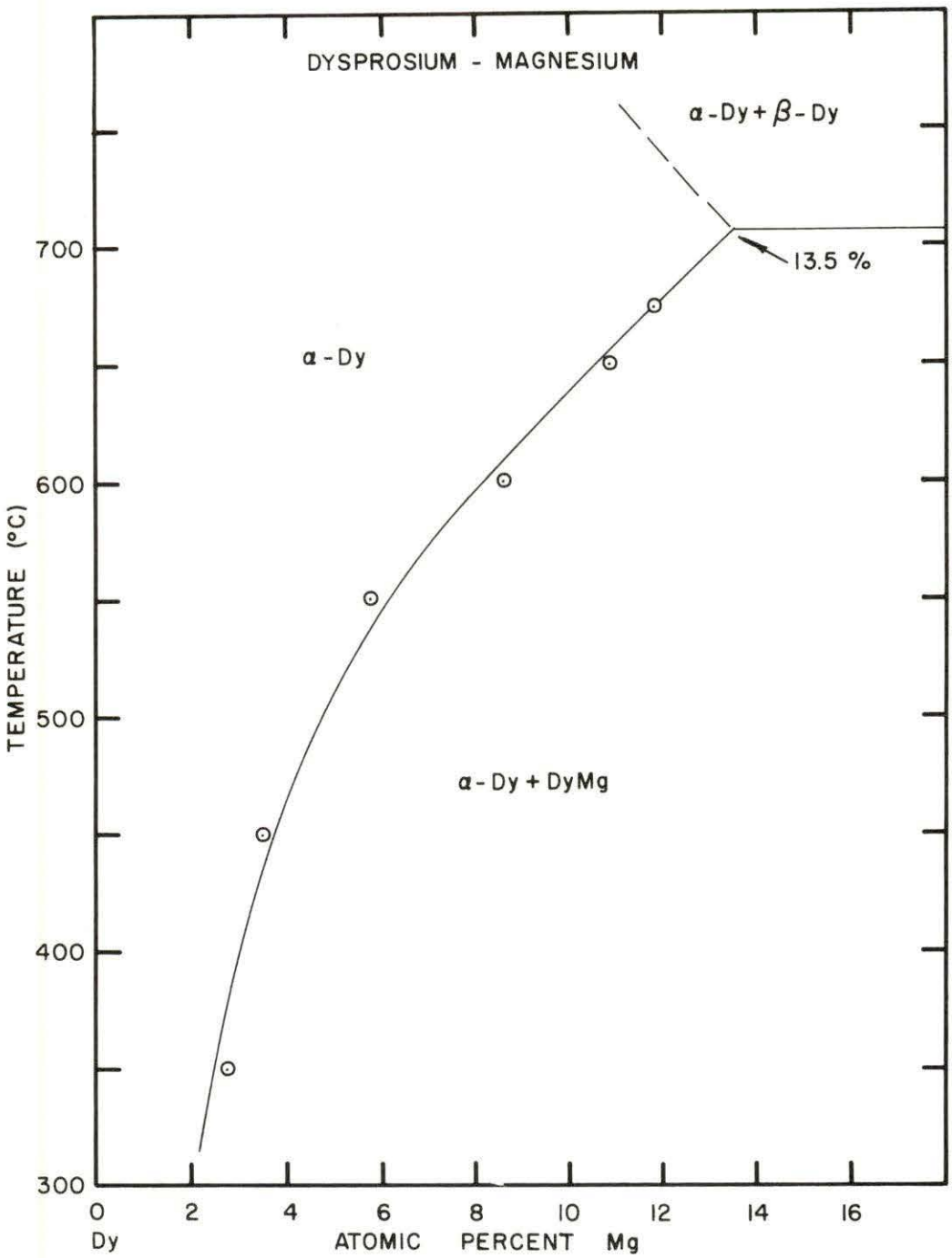

Figure 7. Phase diagram for Dy-Mg system showing solid solubility as a function of temperature

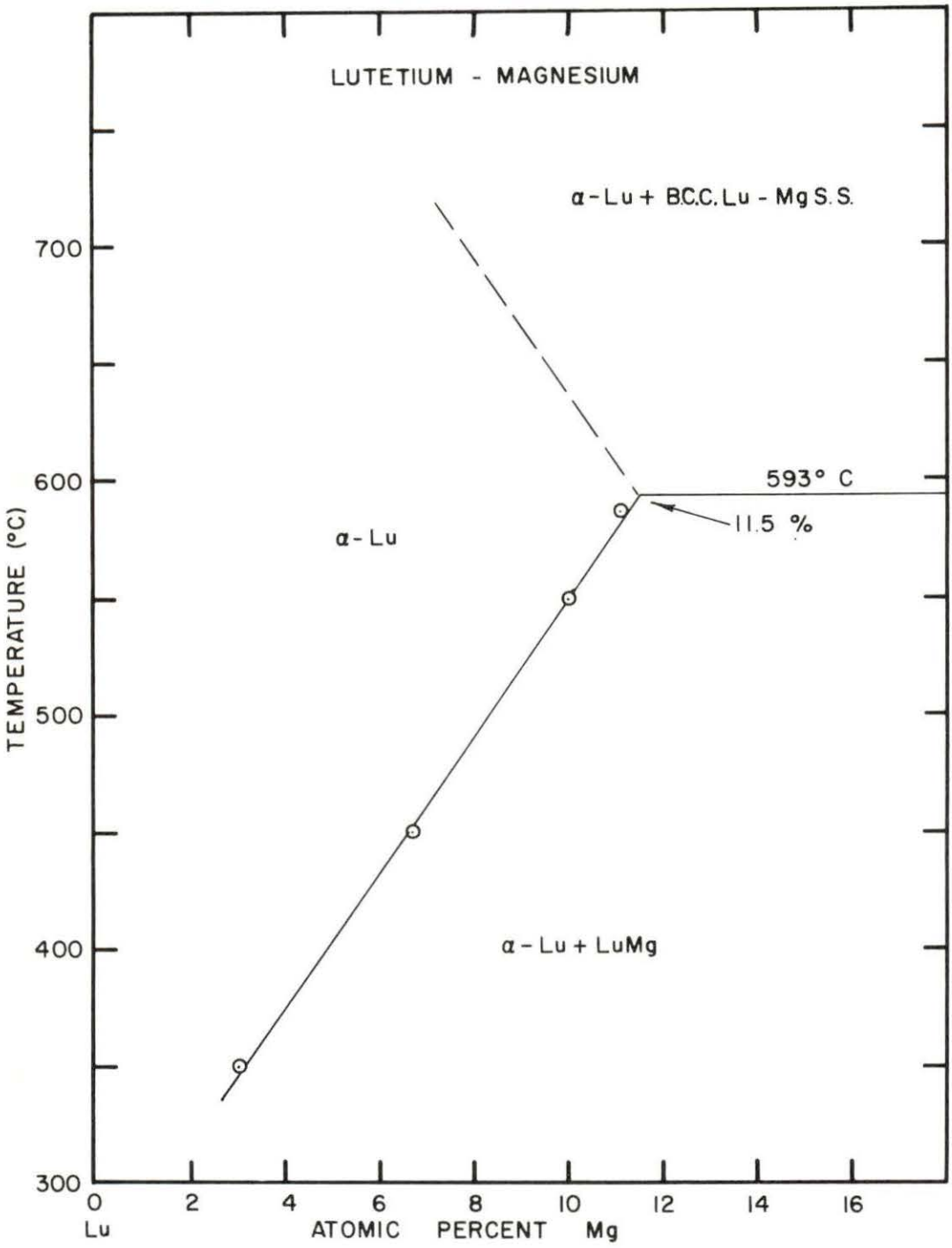

Figure 8. Phase diagram for Lu-Mg system showing solid solubility as a function of temperature

Konovalow thermodynamic relations (23, p. 126) the resulting curve will probably be linear only for solutions which obey Henry's or Raoult's law and have a second phase which is a line compound. The data plotted in this manner showed a tendency to deviate from linearity at low temperature. This may be due to either a departure from ideality at high temperature or to a lack of thermal equilibrium at low temperatures. Because of reasons to be discussed later the solubility data are shown in Figure 9 plotted versus reciprocal homologous temperature, T_m/T, where T_m is the melting temperature of the rare earth solvent.

D. Errors

The precision of any individual determination of a solubility point is not as small as we would have desired. The errors which arise are twofold. The composition of the sample is somewhat in doubt. Even though all components are placed in a sealed crucible the vapor pressure of magnesium is so high at the temperatures at which the alloys were made that an appreciable percentage of the magnesium is in the vapor. Because all of the vapor does not condense back into the alloy on cooling an error in composition results. It is

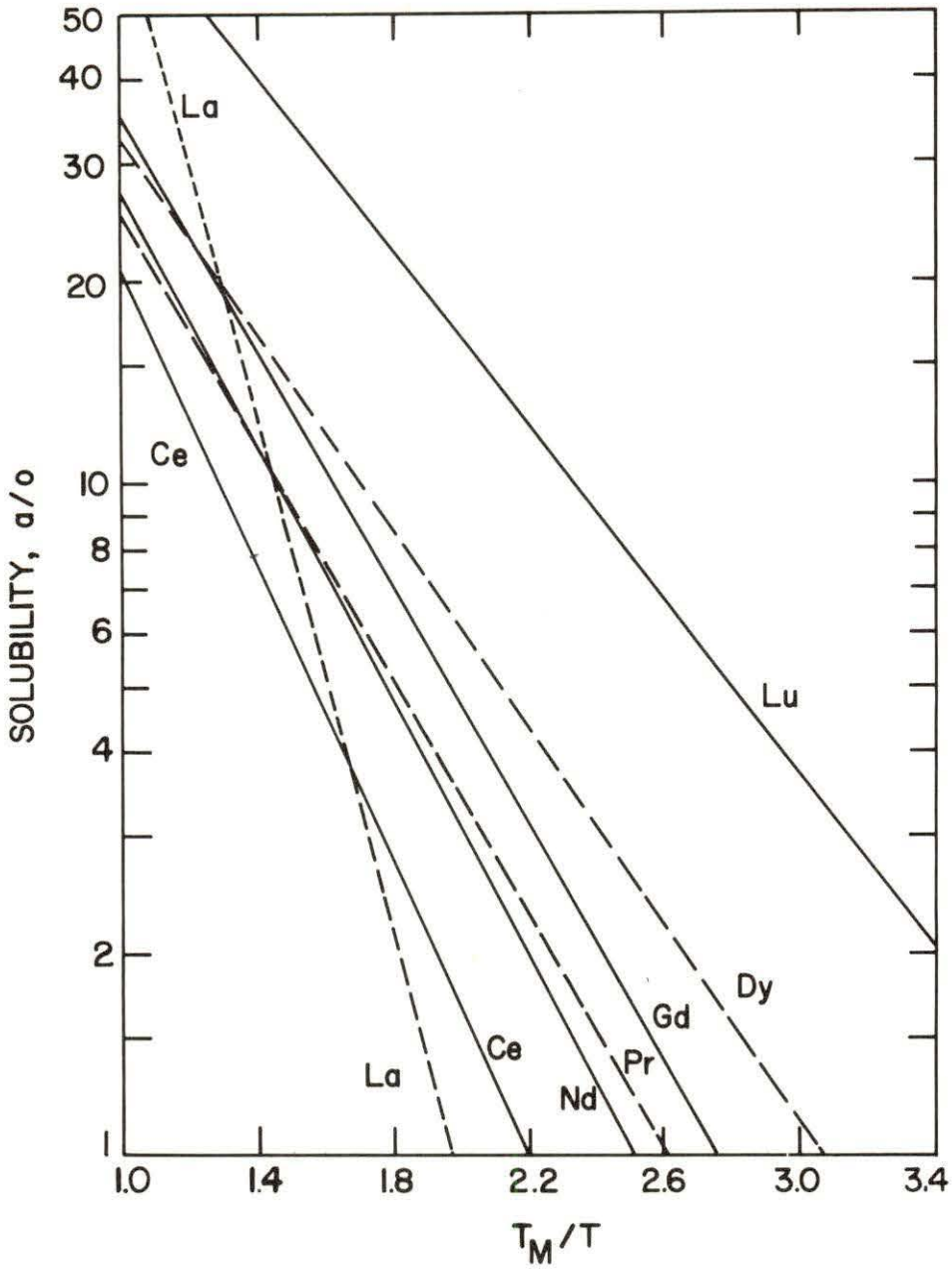

Figure 9. Solubility of magnesium versus reciprocal homologous temperature. Curves include an extrapolated portion for temperatures higher than eutectoid temperatures

estimated that this will shift the composition to lower magnesium concentrations by about .1 atomic percent for lanthanum and successively larger amounts as we proceed along the rare earth series to .3 atomic percent for lutetium, the last member. Also the loss of magnesium from the filings will cause a shift in composition but this is expected to be small since filings are heat treated at a comparatively low temperature. A certain random error is introduced in the determination of the lattice parameter from the x-ray patterns but this error is not expected to have much effect on the final solubility curve since the standard deviation of the lattice parameters is small.

The annealing temperature of the filings was only controlled to $\pm$ 2½°C. This would not introduce any error into the lattice parameter versus composition curve but it might cause the solubility determination to be in error by $\pm$ .1 atomic percent. Impurities would not be expected to greatly effect the solubility data but it was apparent in the lutetium data that some impurity in the "pure" metal had an effect on the lattice parameter, since the unit cell volume per atom was found to increase as the annealing temperature was increased. (See Figure 3) It is not known what effect

if any this impurity had upon the solubility, but it is assumed to be small because the solubility is in line with that of gadolinium and dysprosium.

IV. DISCUSSION

As explained in the introduction several authors have tried to explain the causes of the deviations from Vegard's "law" that are usually found in solid solution alloys (3)(5). These theories predict a deviation from Vegard's "law" at specific composition so it is possible to make an extrapolation from dilute rare earth solutions to 100% magnesium to give an apparent atomic size for magnesium.

The above extrapolations were programmed for the 7074 computer for both the first and second order elasticity theories. Figure 10 and Table 2 show the results of these extrapolations for the first and second order elasticity theory correction. The data in Figure 10 are plotted as size factor (AR-AAR/AR) versus atomic number of the rare earth

AR = atomic radius of rare earth

AAR = apparent atomic radius of magnesium

metal. In addition to the first and second order terms another size factor based upon the sum of the first and second order terms is also shown. These theoretical size factors are compared with the experimental size factors obtained by extrapolation of the experimental volume versus composition plots Figures 2 and 3 to 100% magnesium. It

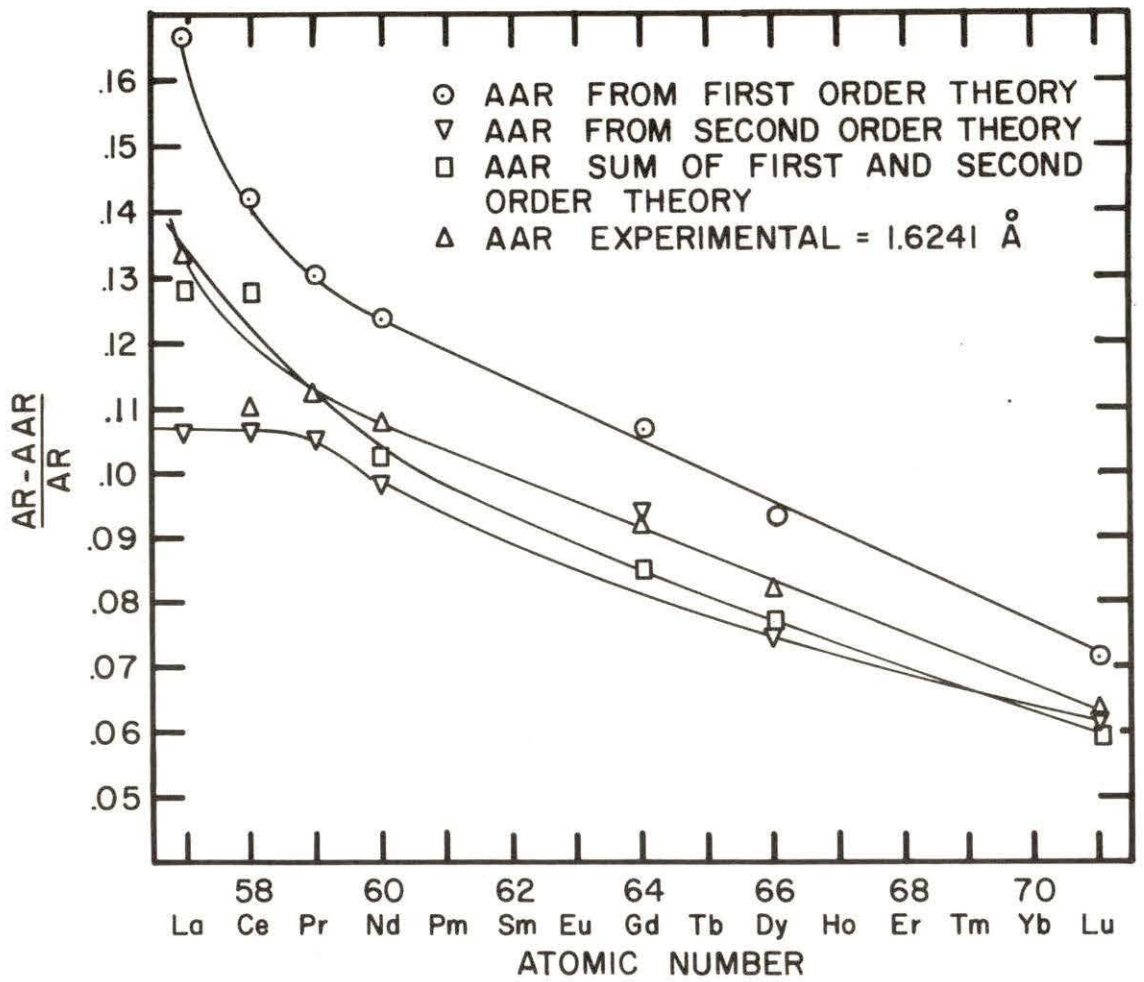

Figure 10. **Size factor (AR-AAR/AR) versus atomic number of rare earth solvent for first and second order elasticity and experimental values of AAR**

Table 2. Apparent atomic radius of magnesium

	AAR calculated from 1st order elasticity	AAR calculated from 2nd order elasticity	AAR from sum of 1st and 2nd order elasticity	AAR from experimental data
La	1.5628 Å[a]	1.6752 Å	1.6360 Å	1.6970 Å
Ce	1.5652	1.6298	1.5920	1.6266
Pr	1.5898	1.6337	1.6215	1.6158
Nd	1.5954	1.6404	1.6340	1.6174
Gd	1.6088	1.6314	1.6382	1.6319
Dy	1.6083	1.6399	1.6365	1.6080
Lu	1.6112	1.6268	1.6320	1.6465

[a]The data in this table are not known to the precision listed here. But because of the difficulty in determining how many significant figures are correct they have been listed with the same number of significant figures as the data from which they are calculated.

was felt that because of the long extrapolation the values of AAR of magnesium determined from the experimental data could only be justified as being constant for all of these alloys. The individual values with the exception of the value for the lanthanum alloys were averaged to give a constant experimental AAR of 1.6241 Å as compared to 1.6020 Å for pure magnesium. It can be seen from Figure 10 that the size factor calculated from the sum of the first and second order corrections agrees best with the experimental data.

At first glance the solubility data summarized in Figure 11 do not appear to be related to any of the usual factors such as the size or atomic number. The solubility on the basis of a more favorable size factor and also the Darken-Gurry technique would be expected to increase in going from lanthanum to lutetium due to the lanthanide contraction and the fact that the radius of magnesium is less than that of the rare earth metals. But from Figure 11 it can be seen that the maximum solubility decreases for the light rare earth metals then it takes a large jump between neodynium and gadolinium, and finally decreases with atomic number for the heavy rare earth metals. These results may seem somewhat surprising due to the fact that there are no electronic

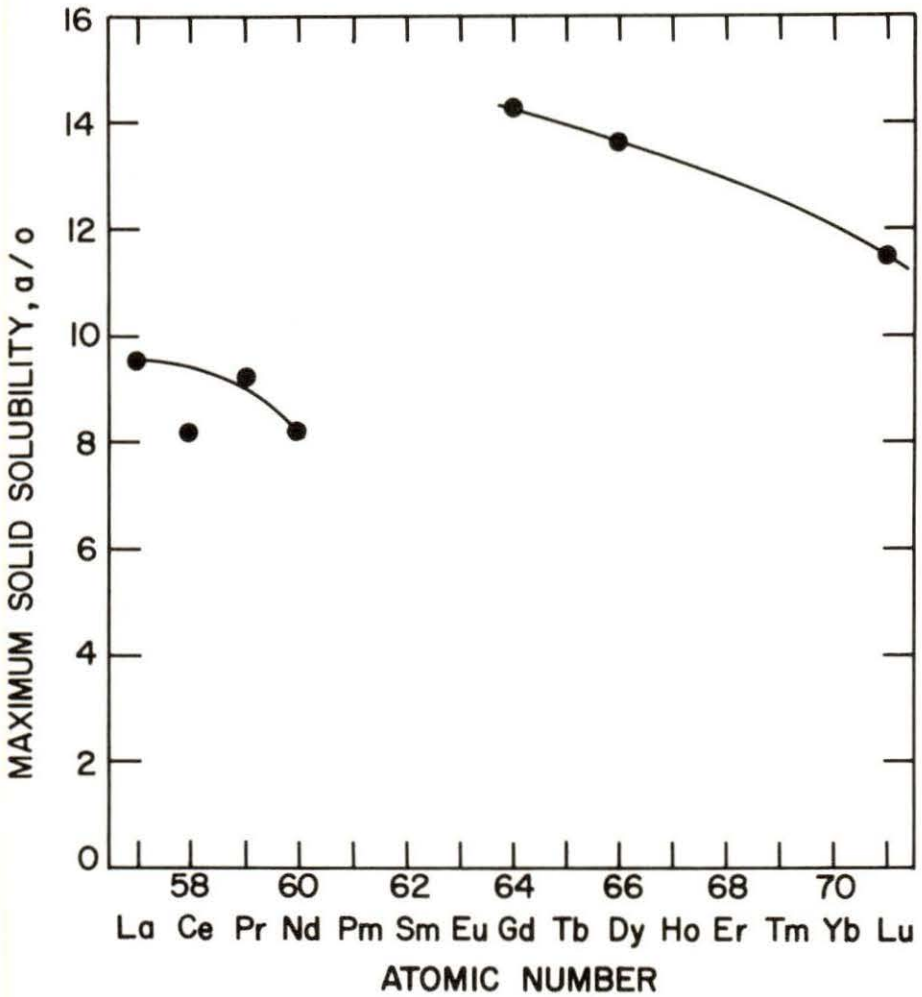

Figure 11. Maximum solubility of magnesium in rare earth metal versus atomic number of rare earth metal

effects to explain this behavior and that the crystal structure remains close-packed even though a change from face-centered cubic to double hexagonal to hexagonal occurs.

This apparent discrepancy can be reconciled if one looks at the solubility at a homologous temperature (temperature of interest divided by the melting point temperature of the rare earth metal). The logarithm of the solubility is plotted versus T_m/T in Figure 9. If the solubility at some fixed T_m/T (Figure 9) is plotted as a function of atomic number it is seen that the solubility increases with increasing atomic number. If the solubility is plotted versus experimental size factor (Figure 12 $T/T_m = .5$) the data fall on a smooth curve. This curve shows that the solubility increased with decreasing size factor. The experimental curve is in good agreement with the curve which was obtained by using the size factor calculated from the sum of the first and second order elasticity theory. The above correlation is not too surprising if one looks at a metal as a set of vibrating atoms which increase in vibrational amplitude as one approaches the melting point. Thus we assume the vibrational amplitude to be approximately equal at the same homologous temperature. Therefore to compare solubilities it is necessary to compare

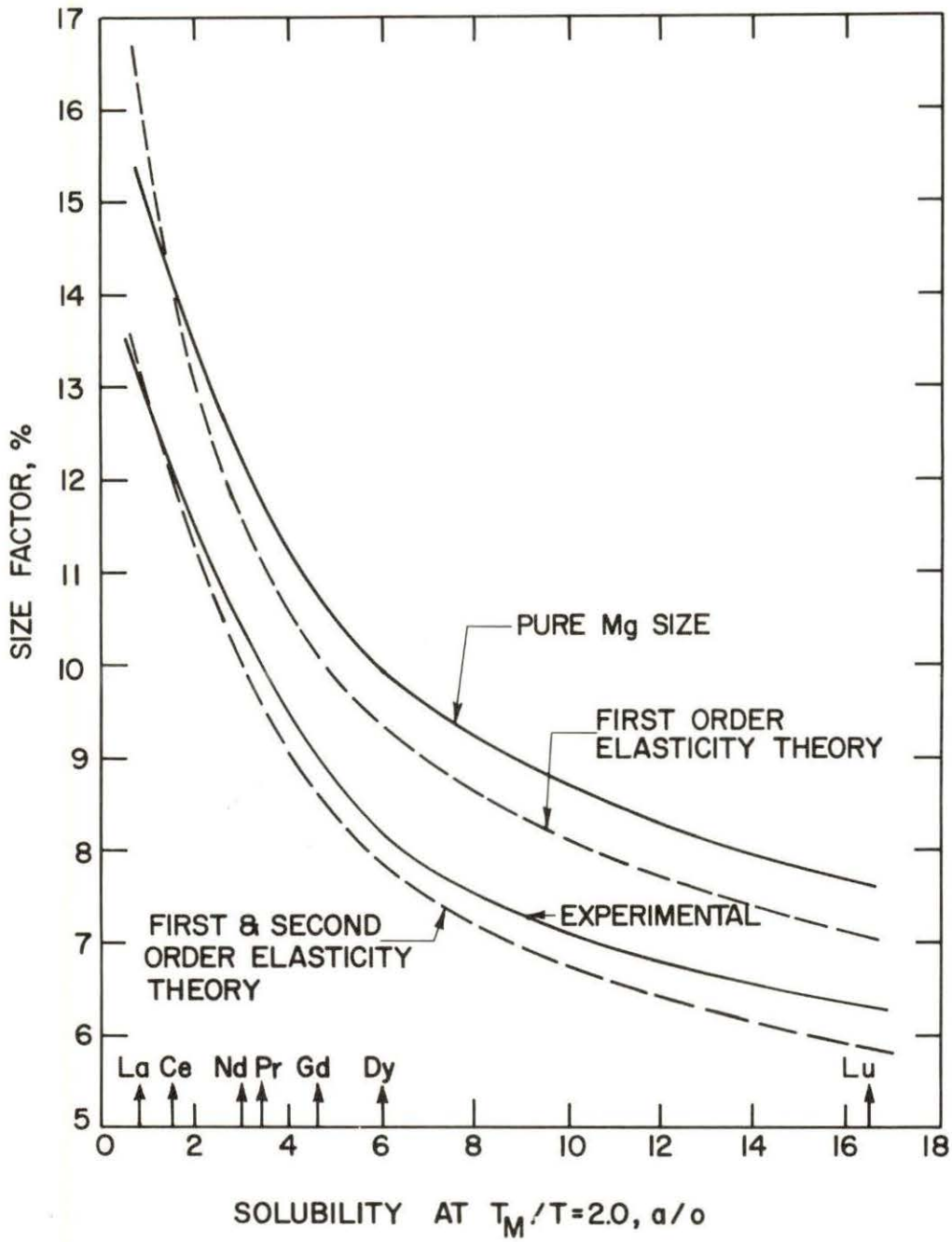

Figure 12. Size factor (AR-AAR/AR) versus solubility of magnesium in rare earth metals at a homologous temperature $T/T_m = 0.5$

at some fixed vibrational amplitude (same homologous temperature) since the vibrational amplitude would be expected to influence the solubility (24, p. 288).

Examination of the variation of the eutectoid temperature as a function of atomic number (lower part of Figure 13) shows a maximum at holmium but the homologous eutectoid temperature shows an approximately linear decrease from lanthanum to lutetium (upper part of Figure 13).

Similarly the melting point or peritectic temperature (17)(18)(19)(20) of the first compound REMg plotted as a homologous temperature versus atomic number shows a similar linear decrease. Another fact is that the free energy of formation for the compound REMg (22) has a tendency to decrease from gadolinium to lutetium. Since it is known (9) that the nature of the second phase effects the solubility it is expected that the above facts and the solubility are interrelated but unfortunately present day theories are not far enough advanced to take all these in account.

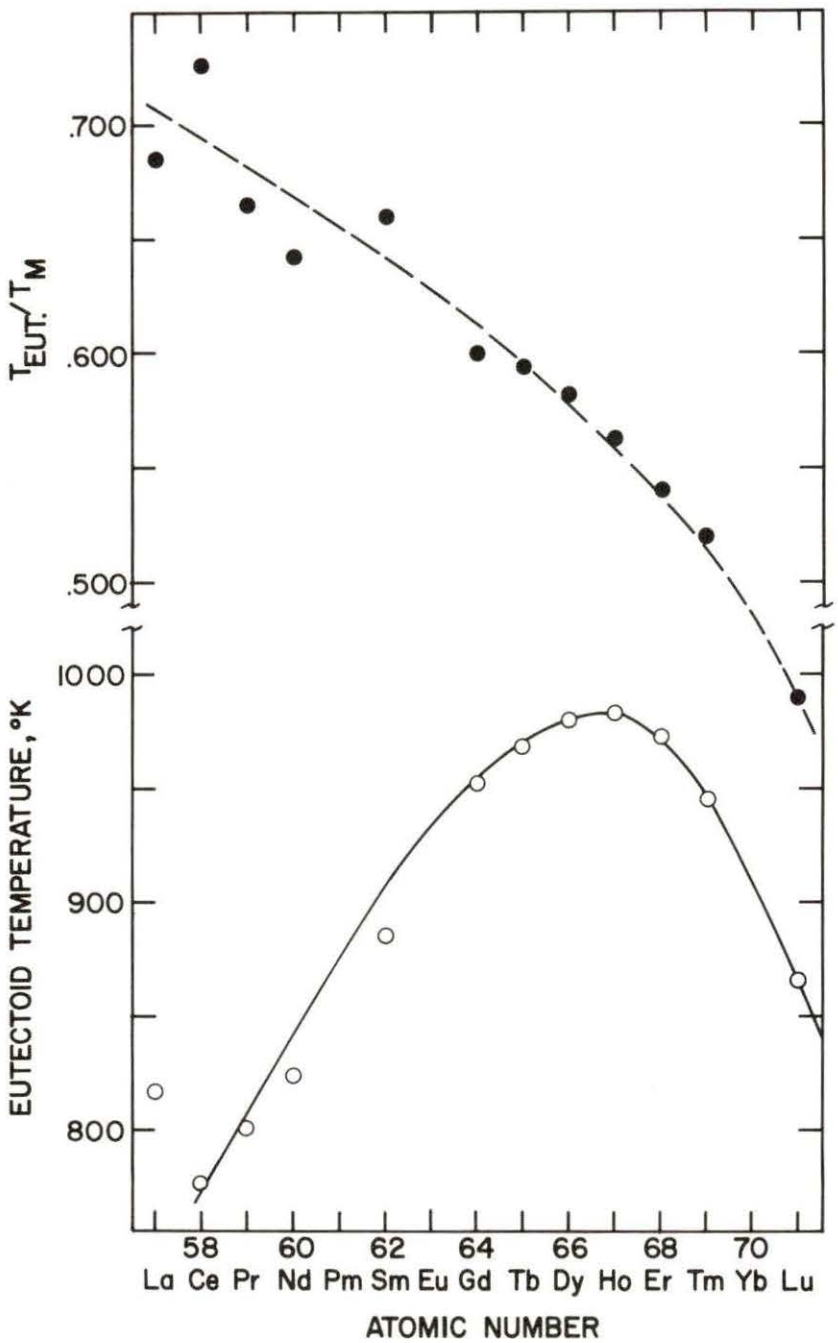

Figure 13. (Upper portion) Homologous eutectoid temperature versus atomic number of rare metal (Lower portion) Eutectoid temperature versus atomic number of rare earth metal

V. CONCLUSIONS

In conclusion the maximum solubility of magnesium in the rare earth metals was found to show an unusual behavior as a function of atomic number of the rare earth metal. For the light rare earth metals it was found to vary from 9.4 atomic percent for lanthanum to 8.2 atomic percent for neodymium and then jump up to 14.1 atomic percent for gadolinium. For the heavy rare earth metals the solid solubility was found to decrease again in a regular fashion. However when the solid solubility was compared at a homologous temperature the solubility was found to increase in a smooth manner with decreasing size factor. It was found that the apparent atomic diameter of magnesium dissolved in the rare earth metals was constant and could be best accounted for by combining the first and second order elasticity theories.

VI. BIBLIOGRAPHY

1. B. L. Averbach: Theory of Alloy Phases, Amer. Soc. Metals, Cleveland, Ohio, 1956.

2. L. Vegard: Z. Physik, 1921, vol. 5, p. 17.

3. J. Friedel: Phil. Mag., 1955, vol. 46, p. 514.

4. P. E. Rider: M.S. Thesis, Library, Iowa State University, Ames, Iowa, 1964.

5. K. A. Gschneidner, Jr. and G. H. Vineyard: J. Appl. Phys., 1962, vol. 99, p. 3444.

6. W. Hume-Rothery and G. V. Raynor: The Structure of Metals and Alloys, 4th ed., Institute of Metals, London, England, 1962.

7. J. D. Eshelby: Solid State Physics, 1956, vol. 3, p. 79.

8. J. Friedel: Advances in Physics, 1954, vol. 3, p. 446.

9. H. Jones: Proc. Phys. Soc., London, 1937, vol. 49, p. 250.

10. L. Darken and R. W. Gurry: Physical Chemistry of Metals, McGraw-Hill, New York, New York, 1953.

11. J. T. Waber, K. A. Gschneidner, Jr., A. C. Larson, and M. Y. Prince: Trans. Met. Soc. AIME, 1963, vol. 227, p. 717.

12. W. Hume-Rothery, G. W. Mabbott, and K. M. Channel-Evans: Phil. Trans. Roy. Soc., London, 1934, ser. A, vol. 233, p. 1.

13. A. B. Pippard: Phil. Trans. Roy. Soc., London, 1957, ser. A, vol. 250, p. 325.

14. T. B. Massalski and H. W. King: Progress in Material Science, 1961, vol. 10, p. 1.

15. R. A. Oriani: National Physical Laboratory Symposium, 1959, No. 9, vol. 1, p. 2a.

16. K. A. Gschneidner: Rare Earth Research, 1964, vol. 2, p. 181.

17. A. E. Miller and A. H. Daane: Trans. Met. Soc. AIME, 1964, vol. 230, p. 568.

18. R. Vogel and T. Heumann: Z. Metallk., 1947, vol. 38, p. 1.

19. R. Vogel: Z. Inorg. Chem., 1915, vol. 91, p. 277.

20. G. Canneri: Met. ital., 1933, vol. 25, p. 250.

21. A. H. Daane: in The Rare Earths, F. H. Spedding and A. H. Daane, Eds., J. Wiley and Son Inc., New York, New York, 1961.

22. J. R. Ogren: Ph.D. Thesis, Library, Iowa State University, Ames, Iowa, 1965.

23. J. G. Kirkwood and I. Oppenheim: Chemical Thermodynamics, McGraw-Hill, New York, New York, 1961.

24. W. Hume-Rothery: Electrons, Atoms, Metals and Alloys, Louis Cassier Co., Ltd., London, England, 1955.

VII. ACKNOWLEDGEMENTS

The valuable time and guidance of Dr. K. A. Gschneidner is gratefully acknowledged by the author as well as the informative ideas and discussions of B. B. Beaudry. Dr. C. P. Kempter of the Los Alamos Scientific Laboratory is thanked for the use of his computer program for the calculation of lattice parameters. The preparation of rare earth metals by P. Palmer and the establishment of a computer program to determine apparent atomic diameters by O. D. McMasters is greatly appreciated. A special note of thanks is due my wife for her support and patience during this investigation.

VIII. APPENDIX

Lanthanum-Magnesium

Composition at.% Mg	Quenching temperature °C	a_o in Å
0.0 (pure La)	350	5.3044 ± 17
1.8	520	5.2955 ± 17
1.8	520	5.2992 ± 8
1.8	520	5.2969 ± 6
4.7	520	5.2828 ± 21
4.7	520	5.2820 ± 20
7.0	520	5.2754 ± 11
7.0	520	5.2702 ± 3
7.0	520	5.2734 ± 22
8.2	520	5.2725 ± 11
8.2	520	5.2704 ± 9
12.5	520	5.2727 ± 9
12.5	520	5.2711 ± 13
10.5	300	5.3011 ± 16
8.2	342	5.2987 ± 22
8.2	382	5.2981 ± 6
7.0	408	5.2913 ± 12
7.0	420	5.2911 ± 9
7.0	450	5.2856 ± 10
8.2	500	5.2809 ± 11
7.0	508	5.2813 ± 6
12.5	530	5.2715 ± 7

Cerium-Magnesium

Composition at.% Mg	Quenching temperature °C	a_o in Å
0.0 (pure Ce)		5.1610 ± 3
2.3	452	5.1492 ± 4
3.7	452	5.1424 ± 3
5.2	452	5.1346 ± 2
7.15	452	5.1313 ± 3
13.0	452	5.1309 ± 5
13.0	200	5.1538 ± 11
13.0	300	5.1487 ± 5
7.15	350	5.1464 ± 4
5.2	350	5.1461 ± 2
13.0	400	5.1393 ± 2
7.15	420	5.1362 ± 7
13.0	475	5.1283 ± 3
7.15	480	5.1254 ± 8
13.0	485	5.1247 ± 1
13.0	495	5.1217 ± 3
13.0	500	5.1223 ± 3

Praseodymium-Magnesium

Composition - at.% Mg	Quenching temperature °C	a_o in Å	c_o in Å
0.0 (pure Pr)		3.6735 ± 10	11.8375 ± 61
2.15	520	3.6654 ± 3	11.8187 ± 20
4.25	520	3.6597	11.7968
7.8	520	3.6402	11.7417
5.75	520	3.6520	11.7810
11.8	520	3.6368 ± 4	11.7445 ± 27
11.8	520	3.6372 ± 4	11.7394 ± 26
15.4	520	3.6379 ± 7	11.7474 ± 44
15.4	520	3.6373 ± 4	11.7362 ± 25
7.8	325	3.6579 ± 5	11.8032 ± 30
11.8	400	3.6501 ± 1	11.7708 ± 2
7.8	405	3.6524 ± 5	11.7827 ± 30
11.8	462	3.6473 ± 3	11.7626 ± 20
15.4	500	3.6409 ± 11	11.7302 ± 73
11.8	500	3.6401 ± 7	11.7325 ± 47

Neodymium-Magnesium

Composition at.% Mg	Quenching temperature °C	a_o in Å	c_o in Å
0.0 (pure Nd)		3.6583 ± 4	11.8035 ± 26
2.0	557	3.6516 ± 2	11.7815 ± 17
3.9	557	3.6433 ± 22	11.7558 ± 150
7.2	557	3.6317 ± 1	11.7238 ± 9
11.5	557	3.6277 ± 12	11.7034 ± 80
15.2	557	3.6285 ± 7	11.7121 ± 50
11.5	200	3.6515 ± 9	11.7885 ± 60
7.2	290	3.6487 ± 4	11.7782 ± 26
11.5	370	3.6462 ± 12	11.7687 ± 81
7.2	400	3.6467 ± 4	11.7679 ± 25
11.5	400	3.6454 ± 14	11.7698 ± 95
7.2	445	3.6437 ± 6	11.7568 ± 42
7.2	500	3.6375 ± 5	11.7376 ± 32
11.5	520	3.6285 ± 8	11.7095 ± 63
11.5	535	3.6318 ± 5	11.7269 ± 34
11.5	530	3.6315 ± 1	11.7222 ± 11
15.2	535	3.6304 ± 10	11.7259 ± 8
11.5	545	3.6294 ± 3	11.7127 ± 21

Gadolinium-Magnesium

Composition at.% Mg	Quenching temperature °C	a_o in Å	c_o in Å
0.0 (pure Gd)		3.6338 ± 6	5.7849 ± 70
2.4	668	3.6293 ± 4	5.7661 ± 20
2.4	668	3.6287 ± 3	5.7669 ± 14
6.0	668	3.6149 ± 3	5.7611 ± 90
6.0	500	3.6166 ± 4	5.7520 ± 21
8.0	668	3.6106 ± 3	5.7379 ± 41
8.0	668	3.6108 ± 3	5.7415 ± 39
11.8	668	3.5933 ± 1	5.7171 ± 34
11.8	668	3.5936 ± 1	5.7239 ± 37
11.8	668	3.6000 ± 1	5.7301 ± 7
13.0	668	3.5944 ± 4	5.7221 ± 26
13.0	668	3.5953 ± 4	5.7217 ± 25
15.1	668	3.5916 ± 2	5.7211 ± 3
15.1	668	3.5925 ± 1	5.7210 ± 8
11.8	350	3.6239 ± 4	5.7609 ± 25
13.0	350	3.6241 ± 5	5.7613 ± 27
11.8	450	3.6215 ± 4	5.7541 ± 24
13.0	450	3.6250 ± 2	5.7612 ± 11
8.0	500	3.6161 ± 1	5.7525 ± 6
15.1	500	3.6155 ± 7	5.7466 ± 42
11.8	500	3.6163 ± 10	5.7522 ± 5
11.8	550	3.6117 ± 3	5.7472 ± 16
13.0	550	3.6131 ± 1	5.7496 ± 8
11.8	600	3.6040 ± 1	5.7331 ± 9
13.0	600	3.6073 ± 1	5.7373 ± 7
15.1	648	3.5985 ± 4	5.7259 ± 7
13.0	648	3.5967 ± 3	5.7205 ± 6

Dysprosium-Magnesium

Composition at.% Mg	Quenching temperature °C	a_o in Å	c_o in Å
0.0 (pure Dy)	698	3.5953 ± 1	5.646 ± 5
5.45	690	3.5167 ± 5	5.6495 ± 7
5.45	550	3.5748 ± 2	5.6405 ± 8
7.9	695	3.5645 ± 4	5.6389 ± 14
10.6	700	3.5616 ± 3	5.6335 ± 22
10.6	695	3.5602 ± 3	5.6337 ± 11
10.6	700	3.5591 ± 3	5.6350 ± 13
12.5	700	3.5520 ± 6	5.6255 ± 5
12.5	695	3.5513 ± 3	5.6249 ± 13
12.5	700	3.5541 ± 3	5.6318 ± 12
12.5	350	3.5843 ± 2	5.6520 ± 7
12.5	350	3.5863 ± 3	5.6535 ± 11
10.6	350	3.5849 ± 20	5.6537 ± 64
12.5	450	3.5819 ± 3	5.6512 ± 10
10.6	450	3.5827 ± 3	5.6521 ± 10
12.5	550	3.5754 ± 2	5.6464 ± 8
10.6	550	3.5745 ± 3	5.6481 ± 11
10.6	550	3.5739 ± 2	5.6452 ± 7
12.5	600	3.5665 ± 6	5.6387 ± 21
10.6	600	3.5658 ± 5	5.6379 ± 17
12.5	650	3.5572 ± 2	5.6367 ± 9
12.5	675	3.5551 ± 3	5.6358 ± 10

Lutetium-Magnesium

Composition at.% Mg	Quenching temperature °C	a_o in Å	c_o in Å
0.0 (pure Lu)	350	3.5047 ± 5	5.5543 ± 5
2.6	350	3.4979 ± 8	5.5540 ± 6
9.2	350	3.4969 ± 4	5.5547 ± 3
15	350	3.4966 ± 11	5.5540 ± 9
0.0 (pure Lu)	450	3.5063 ± 2	5.5562 ± 2
2.6	450	3.5023 ± 2	5.5567 ± 2
6.8	450	3.4949 ± 7	5.5518 ± 7
9.2	450	3.4958 ± 6	5.5572 ± 7
12.7	450	3.4964 ± 9	5.5565 ± 9
0.0 (pure Lu)	550	3.5077 ± 3	5.5589 ± 4
2.6	550	3.5042 ± 7	5.5589 ± 7
6.8	550	3.4902 ± 8	5.5537 ± 8
9.2	550	3.4836 ± 2	5.5479 ± 2
12.7	550	3.4851 ± 9	5.5518 ± 8
15	550	3.4845 ± 5	5.5509 ± 4
0.0 (pure Lu)	585	3.5097 ± 14	5.5585 ± 11
2.6	585	3.5021 ± 12	5.5604 ± 10
3.6	585	3.5011 ± 4	5.5560 ± 4
6.8	585	3.4885 ± 4	5.5496 ± 3
9.2	585	3.4831 ± 2	5.5484 ± 3
9.2	585	3.4858 ± 5	5.5492 ± 4
12.7	585	3.4781 ± 5	5.5437 ± 6
15	585	3.4767 ± 7	5.5487 ± 6
15	585	3.4734 ± 4	5.5416 ± 4